Mechanism of microwave-induced photoluminescence modulation and optically detected resonances due to a two-dimensional electron gas in a heterostructure

I. Baskin, B. M. Ashkinadze, and E. Cohen
Solid State Institute, Technion-Israel Institute of Technology, Haifa 32000, Israel

L. N. Pfeiffer
Bell Laboratories, Alcatel-Lucent Technologies, Murray Hill, New Jersey 07974, USA

(Received 30 June 2008; revised manuscript received 22 September 2008; published 19 November 2008)

The effect of pulsed microwave (mw) irradiation (at 36 GHz) on the photoluminescence (PL) of modulation-doped GaAs/AlGaAs quantum wells (MDQWs) containing a two-dimensional electron gas (2DEG) is studied by time-resolved spectroscopy at an ambient temperature of 2 K. The temporal response of the two-dimensional electron-hole PL to a short mw pulse reveals remarkable PL intensity kinetics with overshoots and a long decay time (>10 ns) after the mw pulse terminates. The observed effects are explained by the temporal evolution of the energy redistribution of photoexcited holes. This redistribution is caused by nonequilibrium, long-lived acoustic phonons that are emitted by the mw heated 2DEG and are absorbed by the holes. Optically detected resonances (ODRs) of the 2DEG are observed in both the two-dimensional electron-hole PL band and in the PL line of excitons that are photoexcited in the undoped superlattice adjoining the MDQW. This provides an experimental proof that the emitted acoustic phonons propagate ballistically throughout the entire heterostructure and induce an effective, long range, indirect interaction between the mw heated 2DEG and the holes (as well as with the spatially separated excitons). This interaction constitutes the underlying mechanism of the mw-induced ODRs observed in heterostructures containing a 2DEG.

DOI: 10.1103/PhysRevB.78.195318 PACS number(s): 73.50.Mx, 78.70.Gq

I. INTRODUCTION

Microwave (mw) or infrared (IR) irradiation of heterostructures containing a two-dimensional electron gas (2DEG) gives rise to remarkable modulation of the resistivity and of the photoluminescence (PL) spectrum.[1–10] Under an external magnetic field, a resonant enhancement of the mw-induced PL (resistivity) modulation occurs and it is studied by optically (electrically) detected two-dimensional-electron (2De) resonances (ODRs): cyclotron, magnetoplasma, and spin.[1–9] The ODR line shape, resonant magnetic field, and linewidth are often used to extract 2DEG properties such as effective mass, mobility, density, and g factor. In contrast to direct mw (IR) resonance detection, ODR is a nonlinear phenomenon since it can only be observed when a 2DEG property is changed under mw (IR) irradiation. The underlying physics of these mw-induced changes is not well understood yet.[5–7,10]

The primary result of the electron-mw radiation interaction is an electron energy increase due to absorption of mw quanta. At low lattice temperatures ($T_L<10$ K), the excess electron energy leads to heating of the entire 2DEG so that the electron temperature T_e exceeds T_L.[11] Similar heating effects occur under high intensity optical or IR illumination,[12,13] as well as under application of a high dc electric field.[14,15] They cause 2DEG mobility reduction and PL spectral changes. While the primary process of mw absorption by the electrons is well understood, the way it leads to PL spectral modulation[16] as well as to resistivity variations[5,6,10] requires further investigation. This is the objective of the present study.

Hot electrons can cause a variety of secondary processes such as electron (hole) and exciton density variations (δn, δn_x),[17–19] an increased population of nonequilibrium low-energy acoustic phonons,[7,20–22] and lattice temperature variations ΔT_L.[1,14] Each mw-induced process has a specific time evolution: T_e and nonequilibrium phonons relax in time scales of 10^{-9} s (Refs. 11 and 23) and 10^{-7}–10^{-8} s,[20–22] respectively. The relaxation times of δn, δn_x are slower ($\sim 10^{-4}$–10^{-7} s).[19,22,24] The bolometric effect relaxation (ΔT_L) is very long.[14] Therefore, studying transient dynamics is important in clarifying the physical mechanisms that govern the effects caused by electron heating in semiconductor heterostructures.

Here, we report on a detailed study of time dependent mw-modulated photoluminescence (MPL) and ODRs in heterostructures containing a modulation-doped GaAs/AlGaAs quantum well (MDQW) with a high mobility 2DEG.

Under weak light illumination, 2DEG radiatively recombines with photoexcited free holes (h) in direct, interband optical transitions. The resulting 2De-h PL spectrum is described by the product of the 2DEG energy distribution function (DF) with that of the free holes.[25] Both energy distributions are perturbed by mw irradiation, and we show that the observed mw-induced PL modulation is mainly due to a change in the hole DF. The hole-energy redistribution is caused by nonequilibrium, low-energy acoustic phonons emitted by the mw heated 2DEG.[16]

The time-resolved PL experiments presented in this study show remarkable transient PL intensity kinetics with overshoots and slow decay (>10 ns) after the termination of a short mw pulse. We attribute the observed mw-induced PL kinetics to the temporal evolution of the hole-energy redistribution due to a "hot phonon effect"—increased population of nonequilibrium low-energy acoustic phonons. Thus, an indirect, long-range interaction between the mv-heated

2DEG and the photoexcited holes is mediated by the nonequilibrium phonons. The main result is a net reduction of the hole-energy relaxation rate. We also show that the physical mechanism of all the ODRs arises from the interaction of the nonequilibrium acoustic phonons with either holes in the MDQW or with excitons in adjoining undoped layers of the heterostructure.

The paper is laid out as follows. Section II details the studied samples and experimental methods. In Sec. III, the experimental results for the time-resolved (and cw) mw-induced spectral PL changes are presented. ODRs that are observed in the 2De-h PL of the MDQW as well as in the exciton PL of the adjoining heterostructure layers are considered in Sec. IV. A discussion of the origin of the mw-modulated PL spectrum, transient mw modulation, and the ODR mechanism is given in Sec. V. Conclusions are presented in Sec. VI.

II. EXPERIMENTAL

Time-resolved mw-induced PL modulation was studied in several asymmetrically (single-side) as well as symmetrically (two-side) modulation-doped GaAs/AlGaAs quantum well structures. The samples were grown by molecular-beam epitaxy on (001)-GaAs wafers. The GaAs quantum well (QW) width is in the range 20–40 nm, and the Si δ-doped layer is separated by an AlGaAs spacer whose width varies in the range of 50–100 nm, depending on the doping level. The 2DEG formed in the QW has a density in the range $n_{2D}=(0.2-2)\times 10^{11}$ cm^{-2} and mobility in the range $\mu_e=(2-5)\times 10^6$ cm^2/V s. Some samples also contain two 100 periods of GaAs/AlGaAs (3/10 nm) superlattices (SLs) grown on the two sides of the MDQW, and the mw-modulated PL of these undoped SLs was also studied.

Two types of sample geometries were used: (1) cleaved rectangles that have a typical size of 1.5×3 mm^2 and (2) round mesas with a diameter of 0.5 or 1 mm that were fabricated by surface etching in order to laterally confine the 2DEG. The sample was inserted inside a short-circuited 8 mm waveguide, at the maximum of the mw electric field, which was directed in the 2DEG plane.

The mw radiation at 36 GHz ($\approx$0.17 meV) was supplied by a Gunn diode, and the mw transmission of the sample containing the 2DEG was measured by a diode-detector. The incident mw power was varied in the range of $P_{mw}=(0.01-20)$ mW and it was modulated with a high-speed p-i-n switch that generates mw pulses with rise and fall times of 5 ns. The mw pulse duration and modulation frequency were varied in the range of $(4\times 10^{-8}-10^{-3})$ s and $f=1$ kHz–5 MHz, respectively.

Photoexcitation and PL detection was done through a small hole in the waveguide. A laser diode with photon energy of $E_L=1.56$ eV (below the AlGaAs band gap) illuminated the sample at incident light intensity $I_L<100$ mW/cm^2. Some of the experiments were preformed under an external magnetic field B that was applied perpendicularly to the 2DEG layer and was scanned in the range of 0–0.4 T. We note that the 2DEG cyclotron resonance (CR) is at $B_{CR}=0.085$ T, corresponding to the electron effective mass of $0.067m_0$ and the used mw frequency. The experiments were done at $T_L=2$ K, and the sample was immersed in liquid He.

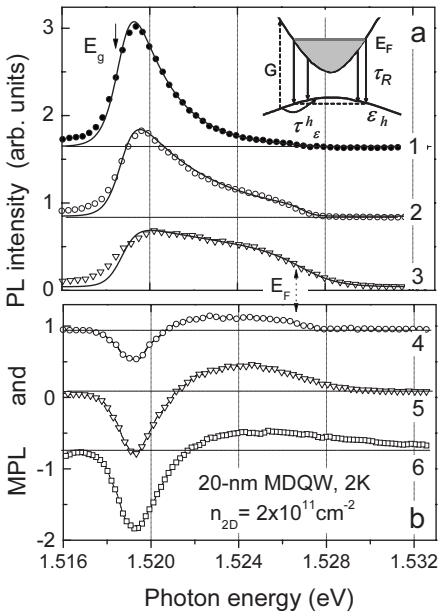

FIG. 1. The 2De-h photoluminescence (a) and microwave-modulated PL (b) spectra ($T_L=2$ K). Curve 1 was obtained without mw irradiation, and all other with cw mw power of: $P_{mw}=0.5$ mW—curves 2 and 4; $P_{mw}=2$ mW—curves 3 and 5; $P_{mw}=20$ mW—curve 6. Inset: a schema of 2DEG-hole optical transitions where G is photogeneration, and ε_h shows a highest energy of the holes recombining with the 2DEG. τ_ε^h and τ_R are the relaxation and 2DEG-h recombination times, respectively. The solid lines in (a) display the PL spectra calculated using Eq. (1) with the fixed values of $E_F=7.2$ meV, $\Gamma=0.7$ meV, $m_h=0.35m_0$, and with the following T_e and T_h fitting parameters: 1.9 and 2.5 K (curve 1); 3.4 and 4.9 K (curve 2); 9 and 20 K (curve 3).

The PL was analyzed by a spectrometer with spectral resolution of 0.1 meV. The signal was detected by a cooled photomultiplier having a response time of 2 ns. A study of mw-modulated PL (MPL) was performed either with a two channel gated photon counter or using the time correlated single-photon counting technique. In the first method, the MPL spectra and ODR traces were obtained by subtracting the PL intensities obtained under mw radiation from those measured at $P_{mw}=0$. The temporal evolution of the MPL intensity change at a monitored photon energy E_m was studied by using the second technique.

III. CW AND TRANSIENT MW-INDUCED PHOTOLUMINESCENCE MODULATION

All the studied MDQWs showed similar mw-induced PL modulation effects. Figures 1(a) and 1(b) present typical PL and MPL spectra obtained for a 20 nm wide MDQW containing a 2DEG of $n_{2D}=2\times 10^{11}$ cm^{-2}. The PL spectrum without mw irradiation [Fig. 1(a), curve 1] is typical of 2De-h recombination of a high mobility 2DEG with a very small density of photogenerated electrons and holes Δn, $\Delta p \ll n_{2D}$. The full width of the spectrum is 7.2 meV

which is close to the Fermi energy E_F for the given n_{2D}. The PL band has a strongly asymmetric shape, indicating that the photoexcited holes relax toward lowest-energy valence-band states and radiatively recombine with the 2DEG in direct optical transitions.

The 2De-h PL spectrum is modified with increasing P_{mw} as shown by curves 2 and 3 in Fig. 1(a). The corresponding MPL spectra are shown by curves 4 and 5 in Fig. 1(b). Under mw irradiation, the PL intensity decreases in the low-energy part of the PL spectrum (negative MPL signal) and increases (positive MPL signal) at higher photon energies, both below and above E_F. It should be noted that the steady state, integrated 2De-h PL intensity does not change under cw mw irradiation[16] in the power range $P_{mw} < 10$ mW.

Similar MPL spectra are also obtained under a perpendicularly applied magnetic field that is equal to the 2DEG cyclotron resonance field B_{CR}. In this case, the mw power P^B_{mw} required to obtain the MPL spectrum coinciding with that measured at $B=0$ is much lower than P_{mw} (by ~40–200 times). From this observation we conclude that the primary cause of 2De-h PL modulation is mw heating of the 2DEG since the mw absorption by the 2DEG is highest at $B=B_{CR}$.[19]

Microwave heating raises the electron temperature T_e and affects mainly the electron distribution near E_F. Therefore, the negative MPL signal in the low-energy spectral part ($E \ll E_F$) and the positive MPL signal around E_F cannot be explained by the sole effect of rising T_e. It must be due to a decreased (increased) hole population of low (high) energy valence-band states as the 2DEG is heated by mw irradiation. Therefore, the observed mw-induced PL modulation results from modification of hole-energy distribution function.

In order to study the underlying mechanism of this mw-induced (secondary) effect, time-resolved experiments were performed in two time ranges. First, MPL spectra were measured at various modulation frequencies of P_{mw} (in the range of $f=100$ Hz–0.4 MHz). It was observed that the MPL spectrum and its intensity were independent of f in a wide range of P_{mw} (<10 mW) and were similar to those shown in Fig. 1(b). Therefore, any MPL intensity relaxation process must be faster than 2 μs. Second, the temporal evolution of the PL spectrum under short mw pulses (of 100 ns duration) and repetition rate of 0.5–2 MHz was studied.

Representative time-resolved PL spectra under mw pulse irradiation are shown in Fig. 2. These were obtained with a 2 ns gate at various time delays relative to the leading mw pulse edge (as shown in the inset of Fig. 2). At time delays of −20 or +140 ns and within the mw pulse plateau, the spectra (open and full circles, respectively) are similar to the steady-state PL spectra measured with and without cw mw irradiation. The spectrum marked by stars was obtained when the mw pulse terminates, namely at a time delay of 112 ns. It differs from that obtained at $P_{mw}=0$ in the spectral part of 1.521 eV $< E <$ 1.528 eV while the PL intensity decreases to its steady-state value at $E > 1.528$ eV. Therefore, the hole-energy redistribution caused by mw radiation lasts at least 12 ns after the mw pulse termination. Moreover, as the gate is set closer to the trailing mw pulse edge (time delay of 105 ns), the spectrum (square symbols) shows an additional PL intensity increase at $E < 1.527$ eV when compared to the spectrum under mw pulse (full circles). This gives rise to an

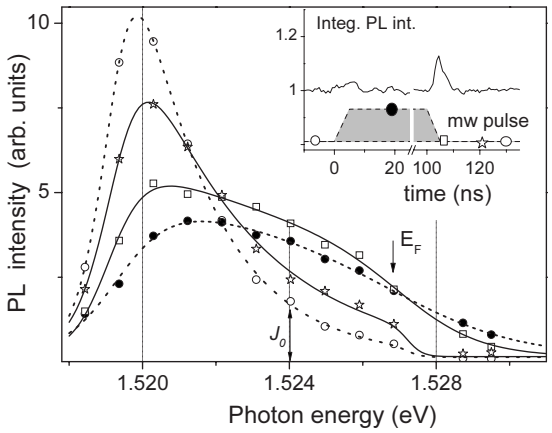

FIG. 2. Transient PL spectra (at $P_{mw} \sim 2$ mW) measured at several delay times relative to the mw pulse leading edge, as shown by the corresponding symbols in the inset. Inset: Temporal dependence of the spectrally integrated PL intensity (solid line) and the mw pulse (dashed line).

increased transient integrated PL intensity when compared with the steady-state value, as shown in the inset of Fig. 2.

The transient PL intensity signals monitored at $E_m = 1.524$ eV (marked J_0 in Fig. 2) are presented in Fig. 3(a) for several P_{mw} values. Curve 1 shows the 100 ns mw pulse measured with a fast mw diode detector. At the lowest absorbed mw power ($P^B_{mw} < 0.05$ mW and $B=B_{CR}$), the PL intensity J (at $E_m=1.524$ eV) increases within the mw pulse duration by a factor of ~2 relative to its value prior to the pulse (marked J_0), and its transient follows the mw pulse waveform as seen in curve 2. As P^B_{mw} increases, the leading and trailing edges of the transient PL signal are modified and intensity overshoots appear in both mw pulse edges [curves 3–5 in Fig. 3(a)]. The overshoot amplitude (e.g., a spike of $\sim 3J_0$ in curve 5) is much higher in the trailing edge. At the same time, the transient PL signal within the mw pulse plateau shows a nonmonotonic dependence on P^B_{mw}: it first increases and then decreases [cf. curves 2, 3, and 5 in Fig. 3(a)]. A similar dependence of the MPL intensity at $E_m = 1.524$ eV on P^B_{mw} is observed in the cw MPL spectra [curves 4, 5, and 6 in Fig. 1(b)].

Remarkable transient PL kinetics are observed around the trailing edge: the intensity increases during ~5–10 ns after the mw pulse terminates and then it decays in the next 10–20 ns. Thus, the PL intensity relaxation becomes significantly longer than the mw pulse fall time.

The transient PL intensity traces monitored at various PL energies are presented in Fig. 3(b). They were measured under $P^B_{mw} \sim 0.3$ mW and $B=B_{CR}=0.085$ T. In order to clearly present the transient intensity changes for various E_m, the PL signal measured before the pulse starts was subtracted and the resulting transient MPL signal was multiplied by the factor shown near the curves in Fig. 3(b). It is observed that a negative MPL signal at low energies, namely, at $E_m \sim 1.520$ eV, has a longer decay than the mw pulse fall time [cf. curve 1 in Fig. 3(a)]. For MPL monitored in the spectral range $E_m \gg E_F$ [at 1.529 eV, in Fig. 3(b)], the signal is positive and its decay time is ~10 ns. For 1.522 eV $< E_m <$ 1.527 eV [Fig. 3(b)], a strong asymmetry is observed be-

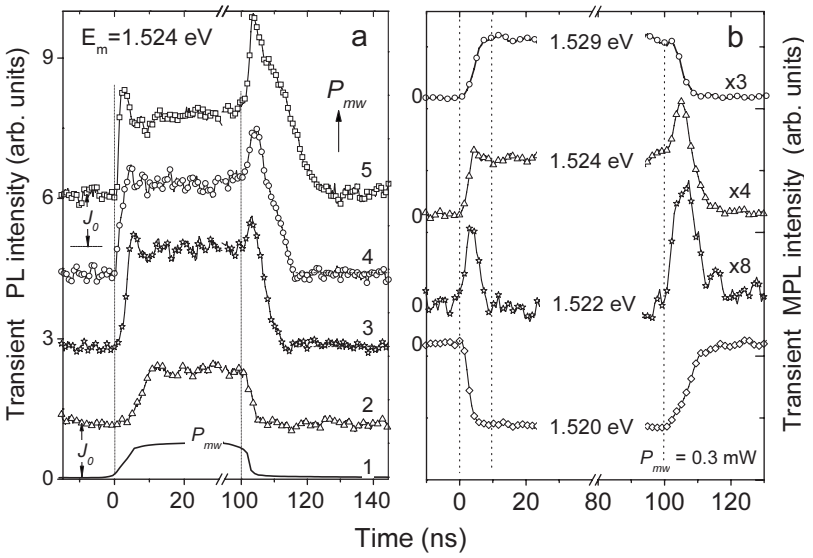

FIG. 3. Transient PL intensity traces measured under a mw pulse (100 ns) at $B_{CR}=0.085$ T. Curve 1 in (a) shows the mw pulse waveform. (a) PL intensity monitored at $E_m=1.524$ eV for the following P^B_{mw}: 0.05 mW—curve 2; 0.2 mW—curve 3; 0.5 mW—curve 4; 1 mW—curve 5. J_0 is the PL intensity at $P_{mw}=0$. (b) Transient MPL intensity monitored at several E_m values and at $P^B_{mw}=0.3$ mW ($B=0.085$ T).

tween the transient intensity signals in the leading and trailing edges.

IV. OPTICALLY DETECTED RESONANCES

The mw-induced PL intensity modulation depends on magnetic field and shows strongest changes at B values where the mw absorption is high. Figure 4 displays the PL intensity dependence on magnetic field $J(B)$ measured under cw mw irradiation (for the same MDQW structure that was used in obtaining Figs. 1–3). The results shown in Figs. 4(a) and 4(b) were measured for two samples: a cleaved rectangular sample and a circular mesa, respectively. The curves at the bottom of the figures display the mw absorption traces obtained from the direct mw transmission measurements using a mw detector $P_{abs}/P_{mw}=(P_{mw}-P_{transmitted})/P_{mw}$.

As described in Sec. II, the MDQW in the studied heterostructures is grown between two supperlattices [marked b-SL and u-SL in the inset of Fig. 4(b)]. Under photoexcitation with a He-Ne laser ($E_L=1.95$ eV), both the 2De-h PL of the MDQW and the exciton PL of the undoped upper SL are observed [upper panel of Fig. 4(b)]. Under cw mw irradiatin PL intensity decreases (increases) in some magnetic field ranges [see Figs. 4(a) and 4(b)], and these are identified as optically detected cyclotronlike resonances (ODRs).[7,8,19]

ODRs occur at the same B values where the mw absorption resonances take place. However, the ODR line shapes [namely, $J(B)$ dependencies] differ significantly from the direct 2DEG mw absorption bands [bottom curves in Figs. 4(a) and 4(b)]. The latter bands are 2DEG dimensional magnetoplasma resonances (DMPRs) that depend on the sample size and shape.[7,19] The DMPR magnetic field value B_R varies with n_{2D} and sample geometry and shifts from the single electron CR $B_{CR}=0.085$ T.[9] Hence, the DMPR mw absorption gives rise to the corresponding ODRs in the $J(B)$ dependence. Several ODR bands as well as several DMPR bands seen in Fig. 4(a) are due to various DMPR modes inherent to the rectangular sample geometry.

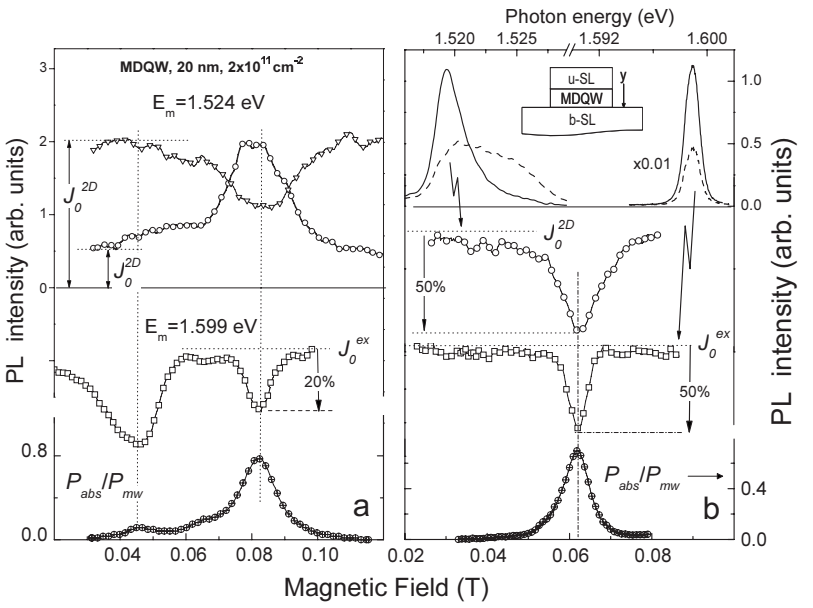

FIG. 4. $J(B)$ (ODR traces) and the mw absorption dependence on B (bottom curves). (a) $J(B)$ traces obtained in a rectangular 2×1 mm^2 sample. Open circles and triangles show the $J(B)$ measured within the 2De-h PL band ($E_m=1.524$ eV) at $P_{mw}=0.02$ and 3 mW, respectively. Square symbols display the $J(B)$ dependence monitored at u-SL exciton PL line ($E_m=1.599$ eV, $P_{mw}=0.2$ mW). Top panel of (b) displays the sample structure containing the MDQW between two SLs. The corresponding 2De-h and exciton u-SL PL spectra are obtained at $P_{mw}=0$ and 0.05 mW. (b) $J(B)$ dependencies measured at $E_m=1.524$ eV and $E_m=1.599$ eV in a mesa sample of 0.5 mm diameter. J_0 is the PL intensity at $P_{mw}=0$. Bottom curve is the corresponding mw absorption trace.

The curves shown by circular and triangular symbols in Fig. 4(a) were measured at the same 2De-h PL energy for two P_{mw} values. They demonstrate the strong nonlinear effect of increasing P_{mw} on the ODR line shape: broadening and sign reversal. Pronounced resonant changes are also detected in the exciton PL of the upper-SL at $E_m=1.599$ eV: its intensity decreases as the mw absorption increases. As shown in the top panel of Fig. 4(b), the exciton PL line shape, however, is not modified under mw irradiation.

For the mesa sample [Fig. 4(b)], only the main DMPR mode is excited and all the traces demonstrate a single ODR resonance band. The $J(B)$ dependence of the 2De-h and exciton SL PL (circles and squares, respectively) shows their ODR at the same $B_R=0.062$ T, and therefore, both ODRs are caused by mw absorption by the 2DEG in the MDQW (under DMPR condition). The primary effect of mw absorption by the 2DEG is further tested as follows: the He-Ne laser beam was directed outside the mesa [the point marked y in the inset of Fig. 4(b)] and the exciton PL from the bottom SL was monitored. It does not show any resonant quenching under mw irradiation. Moreover, a noticeable mw modulation of this b-SL PL occurs at a much higher P_{mw} as compared with that of the exciton u-SL PL. The latter modulation is observed at very low P_{mw} ($\sim$0.05 mW) since it is due to mw absorption by the 2DEG.

The integrated exciton SL PL intensity decreases and this means that the mw-induced exciton PL modulation is due to activation of nonradiative recombination channels in undoped QWs (and SL).[17,26] On the contrary, the integrated intensity of the 2De-h PL does not change under mw irradiation [see also Fig. 1(b)] since the 2De-hole recombination is mainly radiative.[16]

Different line shapes are observed for the DMPR detected directly in mw transmission (bottom curves in Fig. 4) and for the ODRs observed in the 2De-h PL and in the exciton SL PL. A significant 2De-h ODR line-shape modification also occurs as either P_{mw} increases or the monitor energy E_m varies (Fig. 4). In addition, the intensity ratio of the two ODR modes [Fig. 4(a)] is different from that seen in the corresponding mw absorption DMPR traces. Such ODR line-shape transformations are due to a nonlinear dependence of the PL intensity on P_{mw} as one can conclude from the MPL curves of Fig. 1(b). Consequently, the 2DEG parameters (mobility, effective mass) that can be extracted from the nonlinear ODRs give only order-of-magnitude estimates.

In the upper SL spatially separated from the 2DEG layer, the excitonic PL detects the 2DEG DMPR mw absorption occurring in the MDQW. This finding and the hole-energy redistribution observed in the 2De-h MPL spectrum [Fig. 1(b)] reveal the long-range effect of mw heated 2DEG. Thus, energy transfer from the hot 2DEG to the holes (excited in the MDQW) as well as to the excitons (excited in SL) occurs by a long-range indirect mechanism mediated by nonequilibrium acoustic phonons emitted by the hot 2DEG. Therefore, the mw absorption by the 2DEG in the MDQW affects the PL bands of the entire heterostructure. At the same time, the inefficient modulation of the PL from the bottom SL when excited outside the mesa, indicates that there is a directional effect of the ballistically propagated nonequilibrium phonons.

V. DISCUSSION

The primary effect taking place in a mw irradiated high mobility 2DEG is absorption of mw quanta (of $\sim$0.17 meV for 36 GHz radiation) by an electron in phonon-assisted indirect transitions (at $B=0$) or in inter-Landau level transitions. Thereafter, the gained energy is quickly redistributed by electron-electron scattering within the entire 2DEG and the 2DEG temperature T_e rises. The energy transfer from the hot 2DEG to the lattice can lead to its temperature increase ΔT_L. Such a bolometric effect is characterized by a long relaxation time ($\tau_L > 10^{-4}$ s), and the ΔT_L value strongly depends on the thermal sample-bath coupling.[14] We observe a very fast PL response (with a characteristic time of $<5\times10^{-8}$ s) to the short mw pulses and therefore, bolometric effects are excluded.

In this section we discuss two effects of mw heating, namely, rising T_e and an increased population of acoustic phonons emitted by the hot 2DEG.[16,20–22] It should be noted that these two effects cannot be separated in the usually studied mw-induced effects on the 2DEG resistivity, such as the electrically detected resonances[1,2,5,6] and mw-induced resistance oscillations.[10] This is because the 2DEG mobility depends on T_e as well as on population of acoustic phonons participating in the 2De-phonon scattering.[11] Our mw-induced PL experiments allow us to separate these two effects, in particular to prove the predominant role of nonequilibrium phonons in the PL changes, and therefore, in the mechanism of the ODRs that are observed in heterostructures containing a 2DEG.

A. Effect of the nonequilibrium phonons on the 2De-h MPL line shape

The 2De-h PL spectrum is well described by the simple model of radiative recombination of 2DEG with free holes (inset of Fig. 1) (Ref. 25)

$$I(E) = A(T_h,T_e)D_\Gamma(\varepsilon_e+\varepsilon_h')f_e(\varepsilon_e)f_h(\varepsilon_h') \propto D(\varepsilon_e+\varepsilon_h')\exp(-\varepsilon_h'/kT_h)\{1+\exp[(\varepsilon_e-E_F)/kT_e]\}^{-1}. \quad (1)$$

Here, it is assumed that photoholes recombine in direct interband transitions between parabolic, isotropic conduction, and heavy-hole (hh1) valence subbands, and the matrix elements for such transitions are independent of the emitted photon energy E. The two-dimensional (2D) joint density of states is $D_\Gamma(\varepsilon_h'+\varepsilon_e)\propto a\tanh[(\varepsilon_h'+\varepsilon_e)/\Gamma]$, where $\varepsilon_h'=\frac{\mu}{m_e}\times(E-E_g')$ and $\varepsilon_e=\frac{\mu}{m_e}(E-E_g')$ are the hole and electron energies, respectively. E_g' is the renormalized band-gap energy and Γ is a phenomenological broadening parameter. $\mu=m_em_h/(m_e+m_h)$ is the reduced electron-hole mass. f_e and f_h are the Fermi and Boltzmann energy DFs for the 2DEG and low-density holes, respectively. They are characterized by effective electron (hole) temperatures T_e (T_h). We observe that the integrated PL intensity $\int I(E,T_e,T_h)dE$ is independent of T_e, T_h and the normalizing constant $A(T_e,T_h)$ ensures it. This means that holes recombine only radiatively and the photoexcited hole density does not vary under mw irradiation.

The Fermi distribution for the 2DEG with the effective temperature T_e is established owing to the fast energy exchange in electron-electron scattering between the dense 2DEG and hot electrons that are photoexcited at high energy or mw heated. The electron temperature is determined by the balance between the energy gain rate due to 2DEG mw absorption and the energy-loss rate by acoustic phonon emission (for $T_e < 10$ K). The latter can be characterized by the energy relaxation time τ_ε^e which is of 10^{-10}–10^{-9} s for the 2De electrons.[11,23] As shown in numerous measurements and estimates, T_e exceeds T_L at gained power as low as $\simeq 10^{-14}$ W/e.[27,28]

A Boltzmann DF for holes is not established since the energy exchange rates due to the hole-hole and 2DEG-hole scatterings are low at low photoexcited hole density. The hole-energy distribution is governed by the competition of two processes: hole recombination with the 2DEG (mainly radiative) at a rate of $1/\tau_R$ and hole-energy loss to the lattice due to inelastic scattering by acoustic phonons (for $T_L < 10$ K). The corresponding hole-energy relaxation time is[11]

$$(\tau_\varepsilon^h)^{-1} = \frac{2^{3/2}\Xi_1^2 m_h^{5/2}}{\pi\hbar^4\rho}\sqrt{\varepsilon_h} \tag{2}$$

and $\tau_\varepsilon^h \sim 2$ ns at $T_h = 2$ K.[29] Here, the deformation potential of the valence GaAs band, $\Xi = 7$ eV is used.

The 2De-h radiative recombination time in MDQWs is $\tau_R \sim 0.3$ ns.[12,13] Thus, $\tau_R < \tau_\varepsilon^h$ and photoholes recombine before they thermalize so that the hole population of the high-energy (hh1) states exceeds that corresponding to an equilibrium Boltzmann DF with $T_h = T_L$. Hence, f_h should be calculated by solving the kinetic equation.[11,30]

Remarkably, the 2De-h PL spectra shown in Fig. 1(a) are well described by the "quasiequilibrium" Boltzmann DF with $T_h > T_L$ even in the absence of mw irradiation (curve 1 and see also Ref. 16). Solid lines in Fig. 1(a) display the spectra simulated according Eq. (1), and the best fitted T_e and T_h values are given in the figure caption.

Thus in the steady state, a finite lifetime of the holes recombining with the 2DEG ($\varepsilon_h \leq E_F \frac{m_e}{m_h}$) can be taken into account by introducing the increased $T_h > T_L$. The similar conclusion follows from numerical calculations of the kinetic equation for excitons interacting with an equilibrium phonon distribution (Fig. 3 in Ref. 30).

The simulated PL spectra of Fig. 1(a) show that both T_e and T_h increase with P_{mw}. Moreover, T_h exceeds T_e and the ratio T_h/T_e increases with P_{mw} [see fitted T_h (T_e) value in Fig. 1(a) and also Ref. 16]. The increasing T_h under mw irradiation is attributed to the hole-energy redistribution caused by nonequilibrium acoustic phonons emitted by the mw heated 2DEG.[16]

The 2DEG at $T_e < 10$ K emits acoustic phonons with energy $\varepsilon_{\mathrm{ph}} \simeq \hbar v_s k_F \approx 0.5$ meV (v_s is the sound velocity of $\sim 3\times 10^5$ cm/s).[7,28] At low T_L, these low-energy phonons ballistically propagate over the entire sample undergoing elastic scattering by defects and heterostructure interfaces. The lifetime of the low-energy phonons τ_{ph} is limited by phonon transmission (Ref. 33) through the sample boundaries and heterostructure interfaces ($\sim 50\%$). In heat-pulse experiments at $T_L = 2$ K long-lived nonequilibrium phonons were observed in time scale of 10^{-6} s for the GaAs sample of 0.3 mm thickness.[21,31–34]

Thus, an increased population of nonequilibrium long-lived acoustic phonons arises in the entire sample. Holes absorb these long-lived phonons, and a hole-energy redistribution occurs with hole population of low-energy (high-energy) states decreasing (increasing).

The direct energy exchange between 2D electrons and holes is not effective because of the large hole/electron mass ratio. Otherwise, the 2DEG-hole inelastic scattering must have equalized the electron and hole temperatures and cause the holes to have a Boltzmann DF. In addition, the energy-transfer rate due to the electron-hole scattering has to strongly depend on the 2DEG-hole separation. Our study of the MDQWs of various thicknesses (as well as symmetrically and asymmetrically doping) does not reveal such a dependence.

The cw MPL spectra presented in Fig. 1(b) can be qualitatively explained by such an *indirect* 2DEG-hole interaction in which the energy transfer from the hot 2DEG to holes is mediated by acoustic phonons.

Below, we show that the studied transient PL kinetics (Figs. 2 and 3) give strong evidence for this mechanism of the mw-induced PL changes.

B. Transient MPL

Figure 2 demonstrates that the 2De-h PL spectra observed after a mw pulse terminates, are different from those observed under steady state conditions. The transient PL intensity traces in Figs. 3(a) and 3(b) show remarkable mw-induced kinetics with overshoots and long decay in the trailing edge. Since the 2De-h PL modulation is mostly sensitive to the hole-energy distribution, we associate the observed long-lived mw effect with a decreased hole relaxation rate caused by the long-lived nonequilibrium acoustic phonons. It is worth to notice that a reduced energy relaxation rate due to an increased population of optical phonons—hot-phonon effect—is a well-known phenomenon observed under intense short-pulsed photoexcitation of semiconductors.[12,13]

Similarly, we attribute the long relaxation time of the transient MPL to the decay time of nonequilibrium acoustic phonons in mw irradiated heterostructures $\tau_{\mathrm{ph}} \sim 10$ ns. This τ_{ph} value is shorter than that of bulk GaAs. This is probably due to additional phonon decay channels in the AlGaAs alloy or on the heterostructure interfaces.[31]

We analyze the PL intensity transients shown in Fig. 3 using the effective T_e, T_h approximation and assuming that these temperatures have relaxation times of τ_ε^e and τ_ε^h, respectively. Then, the $T_e(t)$ and $T_h(t)$ dependencies under a square-shape mw pulse [dotted curve in Fig. 5(a)] are described by curves shown in Fig. 5(a), dashed and solid lines, respectively. Here, we use $\tau_\varepsilon^e = 1$ ns,[11,23] and we put $\tau_\varepsilon^h = 5$ ns because the rising T_e produces an increased population of nonequilibrium long-lived acoustic phonons that determine the $T_h(t)$ relaxation.

In order to simulate the transient MPL signals for a given photon energy E_m, we introduce these $T_e(t)$ and $T_h(t)$ depen-

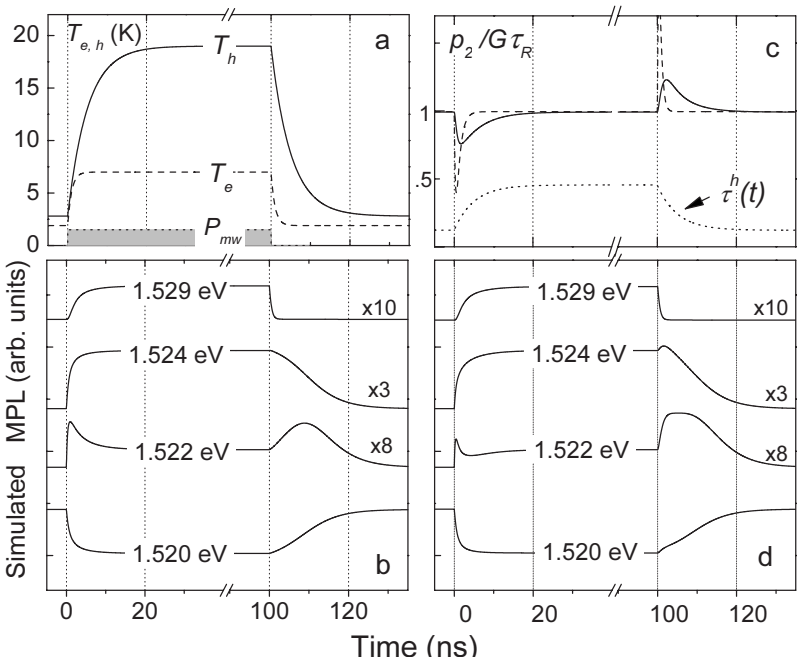

FIG. 5. (a) $T_e(t)$ (dashed curve) and $T_h(t)$ (solid curve) dependencies used in simulation of the transient PL. Dotted curve shows the mw pulse wave form. (b) Transient MPL signals at several PL energies simulated by Eq. (1) and using the $T_e(t)$, $T_h(t)$ dependencies shown in Fig. 5(a). (c) Dashed curve displays the solution of Eq. (3) for the transient "radiative hole" density [Eq. (4)] with $\tau^h(t)$ is taken as the square shaped function (0.5–1 ns). Solid curve presents the numerical solution of Eq. (3), where $\tau^h(t)$ dependence shown by dotted curve was used. (d) MPL transient signals where the transient hole redistribution $p_2(t)$ (c) is taken into account.

dencies into Eq. (1) and calculate the $A(T_e,T_h)(t)$ dependence assuming that the (spectrally) integrated PL intensity is unaffected by the mw pulse application as discussed above. Curves 1–4 in Fig. 5(b) show the calculated transient signals at various E_m, and these reproduce most of the transient PL intensity features shown in Fig. 3(b).

The simulated signals in Fig. 5(b) and the MPL transients in Fig. 3(b) similarly modify with E_m. Indeed, the trailing edge signals in Fig. 5(b) also demonstrate the variable decay kinetics with the overshoots.

Up to now we used the quasiequilibrium steady-state hole (electron) distribution functions with $T_h(t)$ and $T_e(t)$. In this approach, however, the strong amplitude asymmetry in the leading and trailing PL intensity edges [seen in Figs. 3(a) and 3(b)] cannot be reproduced. Below, we propose a model that reveals a specific feature of the *transient behavior* of the nonequilibrium holes that undergo energy relaxation and recombination with the 2DEG. The observed MPL transients asymmetry will be explained by this model.

We consider a simplified model in which the photoexcited hole system is divided into two subsystems having p_1 and p_2 hole densities. The p_1 subsystem consists of the high-energy holes ($\varepsilon_h > E_F \frac{m_e}{m_h}$) that are photogenerated with a rate G and scattered into the p_2 subsystem by acoustic phonons with *a net rate* $1/\tau^h$. We assume that the holes of the p_1 subsystem do not recombine with the degenerate 2DEG. The p_2 subsystem consists of the low-energy holes ($\varepsilon_h < E_F \frac{m_e}{m_h}$) that are generated by the p_1-hole scattering and recombine with the 2DEG. Thus, we have the following system of kinetic equations for two hole subsystems:

$$\frac{dp_1}{dt} = G - \frac{p_1}{\tau^h},$$

$$\frac{dp_2}{dt} = \frac{p_1}{\tau^h} - \frac{p_2}{\tau_R}. \tag{3}$$

Under a mw pulse, the p_2 holes absorbing the nonequilibrium acoustic phonons are transferred into the p_1 subsystem, and the *net* phonon-scattering rate for the p_2-p_1 transitions $(1/\tau^h_{\rm mw})$reduces. Thus, we simulate *the effect* of the mw pulse by a $\tau^h(t)$-square shaped function with $\tau^h_{\rm mw} > \tau^h$. Then, the solution of the kinetic equations [Eq. (3)] has the following forms on the leading (L) and trailing (T) edges:

$$p^L = 1 + \frac{\eta - 1}{\eta - \rho}(e^{-t/\tau_R} - e^{-\rho t/\eta\tau_R}),$$

$$p^T = 1 + \frac{\eta - 1}{1 - \rho}(e^{-\rho t/\tau_R} - e^{-t/\tau_R}). \tag{4}$$

Here, the following dimensionless values are introduced: $p^{L,T} = p_2(t)/G\tau_R$; $\rho = \tau_R/\tau^h$ and $\eta = \tau^h_{\rm mw}/\tau^h > 1$.

The dashed curve in Fig. 5(c) displays the $p_2(t)$ dependence [Eq. (4)] for $\tau^h_{\rm mw}/\tau^h = 2$. This transient curve for the recombining hole density p_2 has very sharp spikes on the pulse edges. The solid curve in Fig. 5(c) is obtained when the time dependent $\tau^h(t)$ value shown by the dotted (bottom) curve in Fig. 5(c) is used in the numerical solution of Eq. (3). Such a $\tau^h(t)$ dependence takes into account that the hole-phonon scattering rate is proportional to the time dependent nonequilibrium phonon population that is assumed to vary similar to the $T_h(t)$ dependence [solid curve in Fig. 5(a)].

The amplitude of the p_2 spikes increases with increased $\tau^h_{\rm mw}/\tau^h$ ratio, as one can see from Eq. (4). At the same time, the steady-state hole density p_2^0 (on the plateau or after the mw pulse) is independent of the τ^h values. This means that the integrated PL intensity (which is proportional to p_2^0) exhibits a transient variation under mw pulse, while it does not change in the steady state. Hence, the assumption of the un-

changed integrated PL intensity that was used above in the analysis of the quasiequilibrium hole system [Figs. 1(a) and 5(b)] does not hold.

Therefore for a nonequilibrium system of holes, a change of the hole-energy relaxation rate results in the transient dependence of the hole density $p_2(t)$ recombining with the 2DEG. Namely, a dip and an overshoot spike appear in the leading and trailing edges, respectively. These features are due to a transient redistribution of holes between "nonradiative-p_1" and "radiative-p_2" subsystems. Since the switching on/off of the mw power is associated with a change in τ^h, the transient hole redistribution should be taken into account.

This was done by multiplying the calculated traces of Fig. 5(b) by $p_2(t)/G\tau_R$. The resulting transients for four PL energies are shown in Fig. 5(d), and these reproduce all the main features of the observed transient PL signals [Figs. 3(a) and 3(b)]. In particular, a remarkable transient PL intensity overshoot asymmetry that increases with increasing P_{mw} [Fig. 3(a)] is obtained in this model. Moreover, as demonstrated in inset of Fig. 2, the transient integrated PL intensity shows a small spike in the trailing edge. Qualitatively, this spike can be understood as due to accumulation of holes in high-energy (nonrecombining) states during the mw pulse and their following relaxation into radiative states. The corresponding dip in the leading edge is not seen in the curve, and this may be due to its small amplitude. It should also be noted that our qualitative model [Eq. (3)] does not take into account all kinetic processes in the nonequilibrium hole system.

C. ODR mechanism

The transient PL study gives conclusive evidence for the nonequilibrium acoustic phonon mechanism underlying the mw-induced PL modulation. These phonons propagate ballistically, and the phonon flux produces a long-range effect on the energy distribution of holes as well as on the PL bands originating elsewhere in the heterostructure.

Under a perpendicularly applied magnetic field, the acoustic phonon flux resonantly increases at the 2DEG CR (or DMPR), and this gives rise to the 2DEG ODR that appears in any PL bands originating in all parts of heterostructure (MDQW, buffer layer,[7] undoped SL, and QWs made of various semiconductor materials[35]). For the studied sample, the long-range effect of the nonequilibrium ballistic phonons leads to a resonant reduction of the exciton PL in the undoped SL [square symbols in Figs. 4(a) and 4(b)]. As these phonons reach the undoped SL, they interact with localized excitons and activate them into delocalized states. Then, the free-moving excitons are captured on traps where they recombine nonradiatively and the PL intensity reduced. Such exciton PL intensity reduction was observed in various structures when a nonequilibrium phonon flux was generated by the heat pulses produced with intense light or dc current.[21,22]

The ODR line shape is nonlinearly modified with increased P_{mw} (Fig. 4). This nonlinearity is determined by the underlying physical mechanism of the ODR and is likely to be caused by a strong dependence of the hole-phonon interaction on the hole energy and on the spectrum of emitted acoustic phonons which varies with increasing electron heating.

The PL modulation studied here provides evidence that an enhanced population of nonequilibrium acoustic phonons is generated and it is stored in the entire sample at very low mw power. Indeed, the mw-induced PL modulation is clearly detected at $P_{\mathrm{mw}} \sim 0.02$ mW. The mw absorption trace shown in Fig. 4(b) allows one to estimate $P_{\mathrm{abs}} \sim 0.5 P^B_{\mathrm{mw}} = 0.01$ mW (at $B=B_R$) that is absorbed by the 2DEG confined in the 0.5 mm diameter mesa. Then, the gained power value per electron is $\sim 10^{-14}$ W/e. At such a low gained mw power, the increased phonon population is well detected by modulation of the 2De-h PL.

VI. CONCLUSIONS

Transient and cw effects of microwave irradiation on low-temperature photoluminescence of heterostructures containing a 2DEG were studied. The observed 2DEG-hole PL spectral change is explained by an energy redistribution of photoexcited holes that absorb nonequilibrium acoustic phonons emitted by the mw heated 2DEG. The mw-induced PL intensity relaxes in ~ 10 ns after the mw pulse termination. Such a long PL relaxation is attributed to a hole-energy redistribution decay which is controlled by long-lived nonequilibrium acoustic phonons.

The transient 2De-h PL dynamics is analyzed using a proposed model that considers the short mw pulse as a source of nonequilibrium phonons that change the hole-energy relaxation rate. This model explains the remarkable PL intensity overshoots at leading and trailing edges of the mw pulse.

Optically detected 2DEG cyclotron resonances are observed within the 2DEG PL band as well as in the exciton PL band originating in the undoped superlattice layers adjoining the MDQW, and this provides further evidence for the long-range interaction mediated by ballistically propagating nonequilibrium acoustic phonons.

Finally, we note that the nonequilibrium acoustic phonons should also affect the 2DEG resistance. Magnetoresistance oscillations caused by increase in mw radiation power, dc current or T_L were recently observed.[10,36,37] All these resistance oscillations occur when phonon population increases due to either enhanced T_L or high mw power (dc current). Probably, phonons generated under these conditions play an important role in the physical mechanism of the magnetoresistance oscillations.

ACKNOWLEDGMENTS

The research at the Technion was supported by the Israeli Science Foundation (ISF) founded by the Israel Academy of Science and Humanities. B.M.A. acknowledges support by a grant under framework of the KAMEA Program.

[1] J. C. Maan, Th. Englert, and D. C. Tsui, Appl. Phys. Lett. **40**, 609 (1982).
[2] D. Stein, G. Ebert, K. von Klitzing, and G. Weimann, Surf. Sci. **142**, 409 (1984).
[3] E. Vasiliadou, G. Muller, D. Heitmann, D. Weiss, K. v. Klitzing, H. Nickel, W. Schlapp, and R. Losch, Phys. Rev. B **48**, 17145 (1993).
[4] N. G. Kalugin, G. Nachtwei, Yu. B. Vasilyev, S. D. Suchalkin, and K. Eberl, Appl. Phys. Lett. **81**, 382 (2002).
[5] E. Olshanetsky, J. D. Caldwell, M. Pilla, Shu-Chen Liu, C. R. Bowers, J. A. Simmons, and J. L. Reno, Phys. Rev. B **67**, 165325 (2003).
[6] J. Matsunami, M. Ooya, and T. Okamoto, Phys. Rev. Lett. **97**, 066602 (2006).
[7] B. M. Ashkinadze, E. Linder, and V. Umansky, Phys. Rev. B **62**, 10310 (2000).
[8] I. V. Kukushkin, J. H. Smet, K. von Klitzing, and W. Wegscheider, Nature (London) **415**, 409 (2002).
[9] B. M. Ashkinadze, A. Nazimov, E. Cohen, A. Ron, and L. N. Pfeiffer, Phys. Status Solidi A **164**, 523 (1997); B. M. Ashkinadze, V. Voznyy, E. Linder, E. Cohen, A. Ron, and L. N. Pfeiffer, Phys. Rev. B **64**, 161306(R) (2001).
[10] M. A. Zudov, R. R. Du, L. N. Pfeiffer, and K. W. West, Phys. Rev. Lett. **90**, 046807 (2003).
[11] S. E. Esipov and Y. B. Levinson, Adv. Phys. **36**, 331 (1987).
[12] J. Shah, *Hot Carries in Semiconductor Nanostructures* (Academic, New York, 1996).
[13] K. Leo, W. W. Ruhle, and K. Ploog, Phys. Rev. B **38**, 1947 (1988).
[14] F. Neppl, J. P. Kotthaus, and J. F. Koch, Phys. Rev. B **19**, 5240 (1979).
[15] J. Shah, A. Pinczuk, A. C. Gossard, and W. Wiegmann, Phys. Rev. Lett. **54**, 2045 (1985); J. Shah, A. Pinczuk, H. L. Störmer, A. C. Gossard, and W. Wiegmann, Appl. Phys. Lett. **42**, 55 (1983); **44**, 322 (1984).
[16] B. M. Ashkinadze, E. Linder, E. Cohen, and L. N. Pfeiffer, Phys. Rev. B **74**, 245310 (2006).
[17] B. M. Ashkinadze, E. Cohen, A. Ron, and L. N. Pfeiffer, Phys. Rev. B **47**, 10613 (1993).
[18] V. V. Bel'kov, J. Hirschinger, D. Schowalter, F. J. Niedernostheide, S. D. Ganichev, W. Prettl, D. MacMathuna, and V. Novak, Phys. Rev. B **61**, 13698 (2000).
[19] B. M. Ashkinadze and V. I. Yudson, Phys. Rev. Lett. **83**, 812 (1999).
[20] M. A. Chin, V. Narayanamurti, H. L. Stormer, and J. C. M. Hwang, in *Phonon Scattering in Condensed Matter IV*, Springer Series in Solid State Science Vol. 51, edited by W. Eisenmenger, K. Lassmann, and S. Döttinger (Springer, Berlin, 1984), p. 328.
[21] A. J. Kent, in *Hot Electrons in Semiconductors: Physics and Devices*, edited by N. Balkan (Oxford University Press, Oxford, 1998), p. 81; A. J. Kent, N. M. Stanton, L. J. Challis, and M. Henini, Appl. Phys. Lett. **81**, 3497 (2002).
[22] A. V. Akimov, L. J. Challis, J. Cooper, C. J. Mellor, and E. S. Moskalenko, Phys. Rev. B **45**, 11387 (1992).
[23] A. A. Verevkin, N. G. Ptitsina, G. M. Chulcova, G. N. Gol'tsman, E. M. Gershenzon, and K. S. Yngvesson, Phys. Rev. B **53**, R7592 (1996).
[24] I. Baskin, B. M. Ashkinadze, E. Cohen, and L. N. Pfeiffer, Phys. Status Solidi C **5**, 131 (2008).
[25] G. A. Bastard, *Wave Mechanics Applied to Semiconductor Heterostructures* (Halsted, New York, 1991).
[26] L. E. Golub, E. L. Ivchenko, and S. A. Tarasenko, Solid State Commun. **108**, 799 (1996).
[27] M. Ari and O. Turkoglu, Physica B (Amsterdam) **348**, 272 (2004); B. K. Ridley, Rep. Prog. Phys. **54**, 169 (1991); H. Çelik, Semicond. Sci. Technol. **17**, 18 (2002).
[28] V. Karpus, Fiz. Tekh. Poluprovodn. (S.-Peterburg) **22**, 151 (1988) [Sov. Phys. Semicond. **22**, 268 (1988)]; Cz. Jasiukiewicz and V. Karpus, Semicond. Sci. Technol. **11**, 1777 (1996).
[29] The holes recombining with the 2DEG have $\varepsilon_h \leq E_F \frac{m_e}{m_h}$ and $\varepsilon_h < 1.3$ meV for the studied samples.
[30] E. E. L. Ivchenko and L. V. Takunov, Fiz. Tverd. Tela (Leningrad) **30**, 1161 (1988) [Sov. Phys. Solid State **30**, 671 (1988)].
[31] K. Wigmore, M. Erol, M. Sahraoui-Tahar, C. D. W. Wilkinson, J. H. Davies, M. Holland, and C. Stanley, Semicond. Sci. Technol. **8**, 322 (1993).
[32] *Phonon Scattering in Solids*, edited by L. J. Challis, V. W. Rampton, and A. F. G. Wyatt (Plenum, New York, 1976).
[33] J. A. Shields and J. P. Wolfe, Phys. Rev. B **50**, 8297 (1994).
[34] M. E. Msall and J. P. Wolfe, Phys. Rev. B **56**, 9557 (1997).
[35] D. Dagnelund, I. Vorona, X. J. Wang, I. A. Buyanova, W. M. Chen, L. Geelhaar, and H. Riechert, J. Appl. Phys. **101**, 073705 (2007).
[36] A. T. Hatke, H. S. Chiang, M. A. Zudov, L. N. Pfeiffer, and K. W. West, Phys. Rev. B **77**, 201304(R) (2008).
[37] M. A. Zudov, I. V. Ponomarev, A. L. Efros, R. R. Du, J. A. Simmons, and J. L. Reno, Phys. Rev. Lett. **86**, 3614 (2001); X. L. Lei, Phys. Rev. B **77**, 205309 (2008).